4.4 NUMERICAL SIMULATIONS OF AIRFLOWS AND TRANSPORT OF AIRBORNE MATERIALS IN THE EXTERIOR AND INTERIOR OF BUILDINGS IN COMPLEX TERRAIN

Tetsuji Yamada*
Yamada Science & Art Corporation, Santa Fe, New Mexico

1. INTRODUCTION

Recently, there have been increasing efforts in combining the CFD (Computational Fluid Dynamics) and atmospheric modeling capabilities to forecast airflows from building scales to terrain scales. This is what is required to simulate airflows over urban areas in complex terrain and/or coastal areas under the influence of mesoscale weather variations.

A typical grid size for a CFD model is 1 m while a typical grid size for an atmospheric model is 1 km. In other words, a difference of three orders of magnitude exists in grid size between CFD and atmospheric models. In addition, CFD models typically provide steady state solutions while atmospheric models deal with diurnal variations. Atmospheric models include water vapor, clouds, and rain, but CFD models do not. Thus, not only grid size, but also model physics are quite different between CFD and atmospheric models

We have added CFD capabilities to a three-dimensional atmospheric model HOTMAC. The new model is referred to as A2Cflow where “A2C” stands for “Atmosphere to CFD.” In this way, A2Cflow can simulate airflows from building to terrain scales in a seamless manner by nesting computational domains. In addition, the model physics become identical for the CFD and atmospheric components since the governing equations are same in a single model.

Affiliated with the A2Cflow is a three-dimensional transport and diffusion code “A2Ct&d” where “t&d” stands for transport and diffusion. A2Ct&d is based on a Lagrangean random walk theory (Yamada and Bunker, 1988). A2Cflow provides three-dimensional mean and turbulence distributions needed for A2Ct&d simulations.

2. MODELS

The governing equations for mean wind, temperature, mixing ratio of water vapor, and turbulence are similar to those used by Yamada and Bunker (1988). Turbulence equations were based on the Level 2.5 Mellor-Yamada second-moment turbulence-closure model (Mellor and Yamada, 1974, 1982). Five primitive equations were solved for ensemble averaged variables: three wind components, potential temperature, and mixing ratio of water vapor. In addition, two primitive equations were solved for turbulence: one for turbulence kinetic energy and the other for a turbulence length scale (Yamada, 1983).

The hydrostatic equilibrium is a good approximation in the atmosphere. On the other hand, air flows around buildings are not in the hydrostatic equilibrium. Pressure variations are generated by changes in wind speeds, and the resulted pressure gradients subsequently affect wind distributions. We adopted the HSMAC (Highly Simplified Marker and Cell) method (Hirt and Cox, 1972) for non-hydrostatic pressure computation because the method is simple yet efficient. The method is equivalent to solving a Poisson equation, which is commonly used in non-hydrostatic atmospheric models.

Boundary conditions for the ensemble and turbulence variables are discussed in detail in Yamada and Bunker (1988). The temperature in the soil layer is obtained by numerically integrating a heat conduction equation. Appropriate boundary conditions for the soil temperature equation are the heat energy balance at the ground and specification of the soil temperature at a certain distance below the surface, where temperature is constant during the integration period. The surface heat energy balance is composed of solar radiation, long-wave radiation, sensitive heat, latent heat, and soil heat fluxes.

Lateral boundary values for all predicted variables are obtained by integrating the corresponding governing equations, except that variations in the horizontal directions are all neglected. The upper level boundary values are specified and these values are incorporated into the governing equations through four-dimensional data

assimilation or a “nudging” method (Kao and Yamada, 1988).

Temperatures of building walls and roofs were computed by solving a one-dimensional heat conduction equation in the direction perpendicular to the walls and roofs. The boundary conditions were a heat balance equation at the outer sides of walls and roofs and room temperatures specified at the inner sides of the walls.

We added a new capability to the A2C modeling system to simulate interactively air flows and transport and diffusion of airborne materials in the exterior and interior of buildings in complex terrain.

3. SIMULATIONS

We selected five (5) simulations to demonstrate the A2C modeling capabilities from a wind tunnel model to atmospheric simulations. Horizontal grid spacing of as small as 1 cm was used.

1. Wind Tunnel Model Simulation

Wind tunnel experiments were conducted under well controlled conditions (in comparison with field campaigns) and extensive measurements were available for verification of model results.

A simulation was conducted in a computational domain of 50 cm x 50 cm x 100 cm (vertical) with horizontal grid spacing of 1 cm. The vertical grid spacing was 1 cm for the first 25 cm from the ground and increased gradually to the top of computational domain.

A model building of 10 cm x 10 cm x 20 cm was placed along the centerline of the computational domain. Fig. 1 shows wind direction (arrows) and wind speed (color) distributions in a vertical cross section along the centerline of the computational domain. Wind direction was westerly (from left to right) and wind speed was 5 m/s in the free atmosphere.

Steady state solutions were obtained when boundary conditions were kept constant and integration continued until flow fields became visibly unchanged.

There was upward motion at the leading edge of the building, which resulted in separation and recirculation of air flows along the roof. Separation of air flows also occurred at the rear side of the building. The modeled characteristics of recirculation and reattachment were in good qualitative agreement with wind tunnel data.

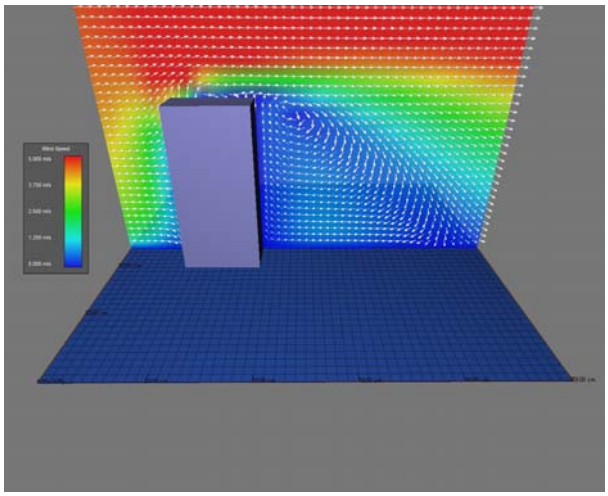

Fig. 1: The modeled wind distributions in a vertical cross section along the centerline of the computational domain

2. Thermal Effect of Building Wall Heating

We investigated thermal effect of buildings on the air flows and transport and diffusion of airborne materials around buildings.

The first case assumed the building wall temperatures were the same as the air temperature adjacent to the walls. The second case represented the afternoon (2 p.m.) condition when the walls facing west were heated by the sun. The third case represented the night time (3 a.m.) condition when wall temperatures were less than the air temperatures adjacent to the walls. Building wall temperatures decreased by long wave radiation cooling.

The computational domain was 200 m x 200 m in the horizontal direction and 500 m in the vertical direction. Horizontal grid spacing was 4 m and the vertical grid spacing was 4 m for the first 15 levels and increased spacing gradually with height. There were 31 levels in the vertical direction.

Two buildings were placed along the centerline of the computational domain. The size of each building was 32 m x 32 m in the base and 30 m in height. Initial winds were westerly and 5 m/s throughout the computational domain Boundary conditions for winds were 5 m/s at the inflow boundary and in the layers higher than 200 m from the ground. Those boundary conditions were maintained through a nudging method.

The initial potential temperature was 25 C at the ground and increased with height with a lapse rate of 1 C/1000 m up to the height 200 m above the ground. The lapse rate increased to 3 C/1000 m in the layer higher than 200 m from the ground. The initial potential temperatures were uniformly distributed in the horizontal direction.

Diurnal variations of building wall temperatures were obtained by solving a one-dimensional heat conduction equation in the direction perpendicular to the wall surfaces. The boundary conditions were the heat energy balance at the outer surfaces and constant temperature (25 C) specified at the inner surfaces.

Fig. 2 shows the modeled wind distributions at 2 p.m. in a vertical cross section along the centerline of the computational domain. The temperature on the wall facing west was approximately 40 C, which was significantly higher than the temperature on the wall facing east (approximately 20 C).

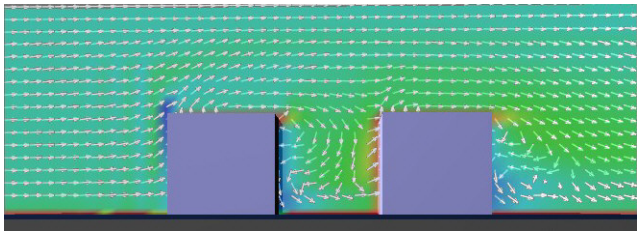

Fig. 2: The modeled wind distributions in a vertical cross section along the centerline of the computational domain at 2 p.m. (Case 2). Arrows indicate wind direction and colors indicate temperatures: red for 40 C and green for 25 C.

Recirculation flows between the two buildings no longer existed. There were upward motions along the warmer walls and downward motions along the cooler walls.

It is obvious from the simulations that air flows around buildings were quite different whether building wall temperatures were higher or lower than the air temperatures. Thermal effects of building walls on air flows were qualitatively verified by observations of soap bubbles released near warm or cold building walls.

To illustrate three-dimensional air flows, particles were released at the ground between the two buildings. Animations will be shown at the presentation.

3. Building Exterior and Interior Airflows

We simulated both exterior and interior airflows of buildings. Two buildings were placed in a computational domain of 200 m x 200 m x 500 m (vertical). Horizontal grid spacing was 4 m and the vertical grid spacing was 4 m for the first 15 levels and increased spacing gradually with height. There were 31 levels in the vertical direction.

Several windows or doors were placed in the building walls so that air could circulate between the exterior and interior of buildings.

Fig. 3 shows modeled particle trajectories. Particles were released at a location inside of upper building and at an upstream side of the entrance of the lower building. Wind direction in the free atmosphere was from left to right (westerly) and wind speed was 5 m/s.

Building walls and roofs were made semi-transparent graphically so that trajectories inside building became visible. The walls and roofs were solid in the simulation.

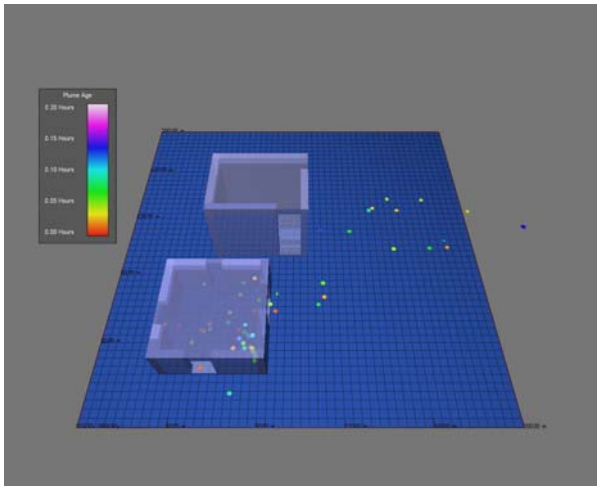

Fig. 3: Modeled particle trajectories released at a location inside of the upper building and at an upstream side of the entrance of the lower building

From the locations and concentration distributions around particles, surface concentration distributions were computed as shown in Fig. 4.

Concentrations were computed by using a Kernel method where concentration distributions were assumed to be normally distributed around the center of each puff (Yamada and Bunker, 1988).

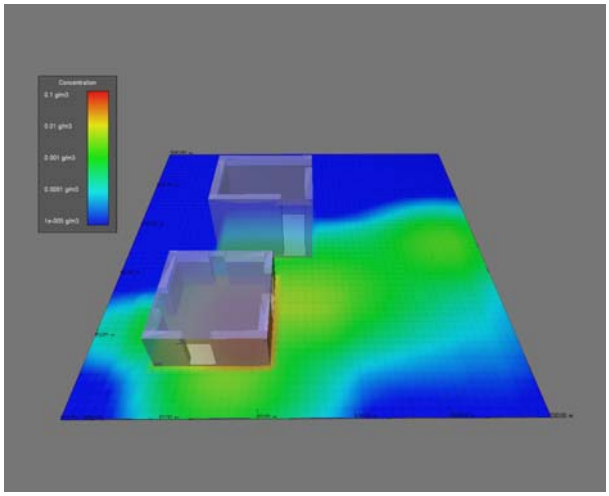

Fig.4: Surface concentration distributions in the interior and exterior of buildings.

4. Building in Complex Terrain

We next considered a case where buildings were located in complex terrain. We used terrain following vertical coordinates to represent accurately topographic variations. The original ground elevation was modified to be flat at building locations similar to cut/fill preparation in actual construction. In this way, the terrain following grid locations at building sites became identical to the Cartesian coordinates. This assured that the building roofs were horizontal.

Fig. 5 shows an example where two buildings were located in a complex terrain. Terrain was cut to flat at building sites so that roofs became horizontal.

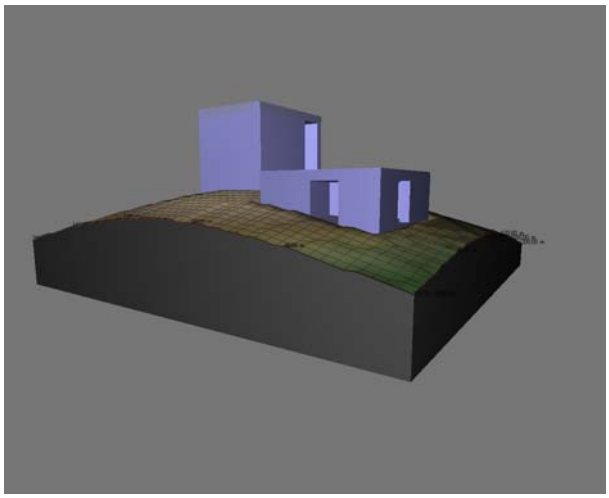

Fig.5: An example where two buildings were located in a complex terrain

Fig.6 shows wind speed (color) and wind direction (arrows) distributions for a simulation in Fig. 5. The computational domain and building locations and size were the same as those in Figs. 3 and 4. The main difference was the underlying topography: flat for Figs. 3 and 4 and Gaussian for Fig. 5 and 6.

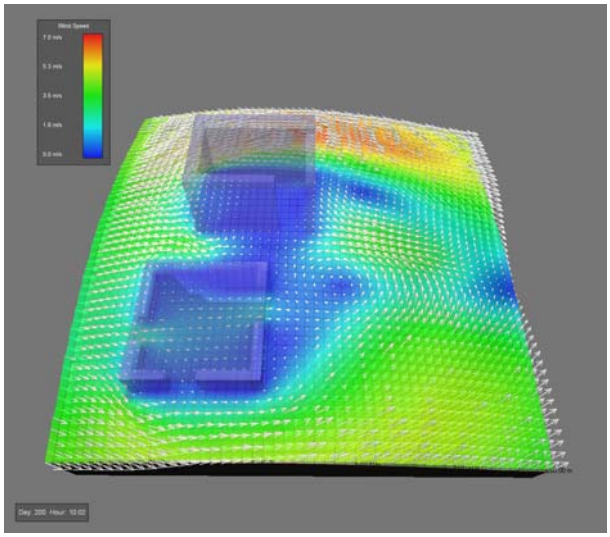

Fig.6: Modeled wind speed (color) and wind direction (arrow) distributions exterior and interior of two buildings in a complex terrain.

5. Nested Grids

We simulated diurnal variations of air flows around a cluster of buildings, which were bound by the ocean and hills (Yamada, 2004). Large cities are often located in a coastal area or near complex terrain. Prediction of transport and diffusion of air pollutants and toxic materials is a considerable interest to the safety of the people living in urban areas.

Two inner domains were nested in a large domain (Fig. 7). The first domain was 6560 m x 8960 m with horizontal grid spacing of 160 m. The second domain was 1280 m x 1440 m with horizontal grid spacing of 40 m. The third domain was 360 m x 400 m with horizontal grid spacing of 10 m.

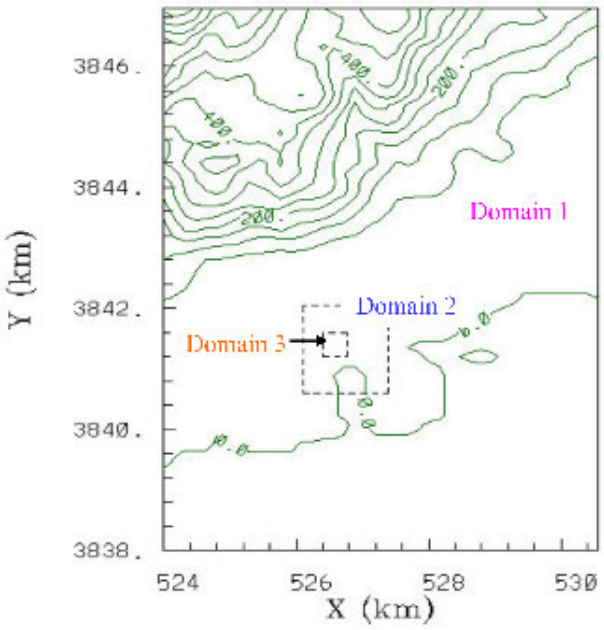

Fig.7: Computational domains: Domain 1 is the outer domain. Solid contour lines indicate ground elevations. Numerical numbers are altitudes in meters. Dashed lines indicate boundaries of nested domains: Domain 2 and Domain 3.

Domain 1 includes topographic features such as the ocean, coastal area, plains, and hills. Domain 2 is a transition area between Domain 1 and Domain 3. Buildings were located in Domain 3.

There were significant differences in wind distributions around building clusters whether building walls were heated or not. Fig.8 shows wind and temperature distributions at 9 a.m. in a vertical cross section of east and west direction.

Arrows indicate wind directions and colors indicate temperatures. Temperatures along the walls facing east were significantly higher than those along the walls facing in other directions.

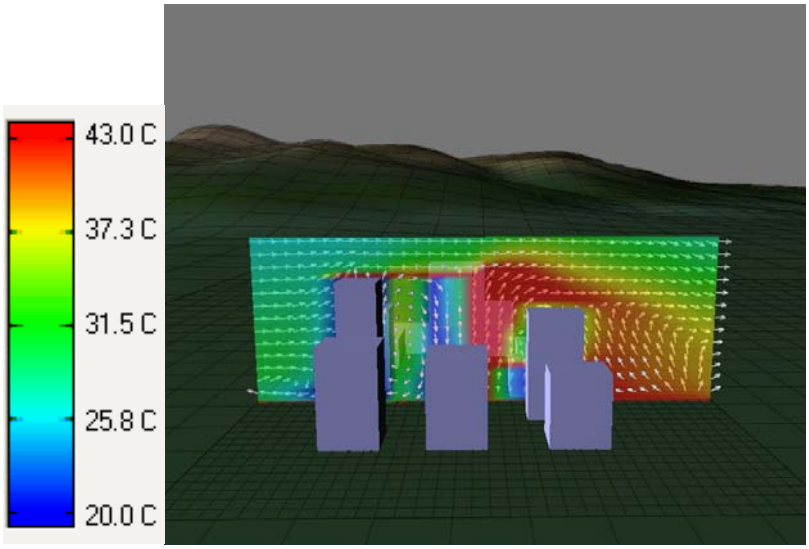

Fig.8: An example of temperature and wind distributions in a vertical cross section in an east-west direction

4. SUMMARY

A three-dimensional atmospheric prediction model, A2Cflow, was improved: airflows not only in complex terrain, but also exterior and interior of buildings and in a wind tunnel were simulated.

We adopted HSMAC method for the non-hydrostatic pressure computation because it is simple yet efficient. The method is equivalent to solving a Poisson equation, which is commonly used in non-hydrostatic atmospheric models.

Airflows around a model building in a wind tunnel were simulated with horizontal grid spacing of 1 cm. Separation and reattachment of air flows at the leading edge and behind buildings were in good agreement of wind tunnel data.

Simulations were conducted to illustrate the thermal effects of building walls on the air flows around two (2) buildings. Building wall temperatures were computed by solving a one-dimensional heat conduction equation in a direction perpendicular to walls. Boundary conditions were a heat energy balance at the outer surfaces of buildings and temperatures specified at the inner surfaces.

When building walls were heated and cooled, air flows around two buildings became quite different from those without wall heating. Recirculation and reattachment around buildings no longer existed. In general upward motions were simulated along warm walls and downward motions were simulated along cold walls.

Airflows exterior and interior of buildings were also investigated. Building interior flows were influenced by the locations of opening (windows and doors) and exterior flows. Exterior flows, on the other hand, were functions of local circulations resulted from topographic variations.

We simulated diurnal variations of air flows around a cluster of buildings, which were bound by the ocean and hills. Large cities are often located in a coastal area or near complex terrain. Prediction of transport and diffusion of air pollutants and toxic materials is of considerable interest to the safety of the people living in urban areas.

There were significant interactions between air flows generated by topographic variations and a cluster of buildings. Sea breeze fronts were retarded by buildings. Winds were calm in the courtyards. Winds diverged in the upstream side and converged in the downstream side of the building cluster.

Wind speeds and wind directions around buildings changed as the winds in the outer domains encountered diurnal variations. Domain 3 alone could not reproduce diurnal variations of winds because it didn't include topographic features responsible for mesoscale circulations such as sea/land breezes and mountain/valley flows.

On the other hand, Domain 1 alone could not depict the effects of buildings because the horizontal grid spacing (160 m) was too coarse to resolve buildings. Air flows around buildings were successfully simulated in Domain 3 and modified air flows in Domain 3 were transferred back to Domain 2 and Domain 1 through two-way nesting algorithm.

A few atmospheric models have both mesoscale and CFD scale modeling capabilities. However, we are not aware of any report that a single model was used to simulate interactions between mesoscale and CFD scale circulations.

Single model approach has several advantages: model physics is identical, interactions are easily investigated by using nested grids, and book keeping associated with code modifications is simple.

REFERENCES

Hirt, C.W., and J. L. Cox, 1972: Calculating Three-Dimensional Flows around Structures and over Rough Terrain. *J. of Computational Phys*., **10**, 324-340.

Kao, C.-Y. J. and Yamada, T., 1988: Use of the CAPTEX Data for Evaluation of a Long-Range Transport Numerical Model with a Four-Dimensional Data Assimilation Technique, *Monthly Weather Review*, **116**, pp. 293-206.

Mellor, G. L., and T. Yamada, 1974: A Hierarchy of Turbulence Closure Models for Planetary Boundary Layers. *J. of Atmos. Sci*., **31**, 1791-1806.

Mellor, G. L., and T. Yamada, 1982: Development of a Turbulence Closure Model for Geophysical Fluid Problems. *Rev. Geophys. Space Phys*., **20**, 851-875.

Yamada, T., 1983: Simulations of Nocturnal Drainage Flows by a q^2l Turbulence Closure Model. *J. of Atmos. Sci*., **40**, 91-106.

Yamada, T., 2004: Merging CFD and Atmospheric Modeling Capabilities to Simulate Airflows and Dispersion in Urban Areas. *Computational Fluid Dynamics Journal,* **13 (2):47**, 329-341.

Yamada, T., and S. Bunker, 1988: Development of a Nested Grid, Second Moment Turbulence Closure Model and Application to the 1982 ASCOT Brush Creek Data Simulation. *Journal of Applied Meteorology*, **27**, 562-578.